Asymptotic Models for Gas–Liquid Crystallization in Two-Film Systems

Michel Cournil and Jean-Michel Herri
Centre SPIN, URA CNRS 2021, Ecole Nationale Supérieure des Mines de Saint-Etienne,
158, Cours Fauriel 42100 Saint-Etienne Cedex 2, France

It is proposed to revisit the problem of gas–liquid crystallization in the framework of a two-film model and with the help of experimental data from two experimental systems. Preliminary quantitative discussion of the order of magnitude of different effects makes possible realistic simplifications in the theoretical models. In particular, the role of the interfacial film in the whole process is clearly defined. As previous researchers have done, a formulation in terms of moments of the crystal size distribution is used; however, instead of the numerical solution to the corresponding differential system, a general procedure to express analytically the asymptotic behavior of the physical system is proposed. With this formulation, the influence of different parameters can be easily identified and validated on the available data from two experimental systems.

Introduction

Gas–liquid crystallization can be described by the overall reaction

$$A_{1\,(\mathrm{gas})} + pA_{2\,\mathrm{aq}} \rightarrow qA_{3\,(\mathrm{solid})} \qquad \text{(R1)}$$

in which $A_{2\mathrm{aq}}$ is a compound dissolved in an aqueous solution, and p and q are stoichiometric coefficients. Gas–liquid crystallization processes are frequently met in industrial or natural systems. This is, for instance, the case of precipitation of gypsum by adsorption of sulfur dioxide into lime water (Sada et al., 1977) and carbonatation of lime water. The latter case has been extensively studied by Wachi and Jones (1991a,b) and Jones et al. (1992), and has given rise to comprehensive interpretations.

Gas hydrate crystallization can be also represented by an [R1]-type reaction in which $A_{2\mathrm{aq}}$ would denote simply water and A_3 the gas hydrate phase (Englezos et al., 1987a,b; Skovborg and Rasmussen, 1994; Herri et al., 1999; Pic et al., 2001).

Models are generally based on the assumption of a two-layer configuration that consists of:

(a) The superficial film at the gas–liquid interface in which absorption and diffusion of the gas into the liquid phase take place (possibly accompanied by reactions between dissolved species); this zone, of both high supersaturation and high concentration gradient values in dissolved gas, is favorable to primary nucleation of crystals;

(b) The bulk zone in which crystals develop mainly by growth; this is a region of lower concentration values and nearly zero gradients, all the more so since the medium is generally stirred.

Classic models take into account:

(1) Basic equations for the gas–liquid mass transfer (film theory) accompanied with kinetic models of chemical reactions;

(2) Equations for the distributed crystal population and dissolved gas mass balances;

(3) Crystallization kinetic laws.

The associated mathematical problem is a partial derivative equation (PDE) problem when simplification cannot be introduced (Wachi and Jones, 1991a,b), or an ordinary differential equation problem when simplifying procedures or assumptions (steady state; use of the crystal population moments) can be applied (Englezos et al., 1987a,b; Herri et al., 1999; Pic et al., 2001).

In this article we would like to revisit several aspects of gas–liquid precipitation in the framework of the two-layer model. Particularly, the different assumptions concerning gas transfer through the interfacial film, crystal growth, nucleation, and transport in this film will be examined. Then, we will propose a general model of crystallization and discuss

some possible simplifications, particularly at later stages of the process. The main originality of this article, however, is to propose analytical laws for the system asymptotic behavior; these predictions can be easily compared to experimental results, and give in several cases a quantitative estimation of the model parameters. This approach, although general, will be supported (and possibly validated) by the experimental context of both calcium carbonate precipitation (Jones et al., 1992) and particularly methane hydrate crystallization (Herri et al., 1999; Pic et al., 2001), for which we have many results.

Models

System configuration

We consider a vertical cylindrical stirred reactor filled with water. The liquid height, volume, and cross-section area are, respectively, denoted by H, V, and A; z is the vertical coordinate (the gas–liquid interface is located at $z = 0$); t is the time. Two zones are considered (Figure 1):

Interface Layer. The interface layer, of thickness δ and volume V' is characterized by a concentration profile $c'(z,t)$ in dissolved gas. The boundary conditions are $c'(0,t) = C_{\text{ext}}$ and $c'(\delta,t) = c_b(t)$; C_{ext} is the gas solubility; $c_b(t)$ is the bulk concentration. The crystal diameter, D, density function should be considered in its local, z-dependent form, $n'(D,z,t)$ expressed per unit volume. Because the agitation state of the interface layer is probably weak, we consider it at rest, as other authors did.

Bulk Zone. Due to the effect of stirring, the concentration in dissolved gas, $c_b(t)$, and the crystal diameter density function per unit volume, $n_b(D,t)$, are considered as independent of z. The agitation state, imposed by the stirrer, is assumed to be uniform and completely characterized by the stirring rate ω or equivalently the mean energy dissipation rate $\bar{\epsilon}$.

In what follows, the superscript prime will be used to denote variables or parameters relative to the surface layer, whereas bulk variables or parameters will be written with subscript b. Variables or parameters without particular indication are relative to the global system or to both zones.

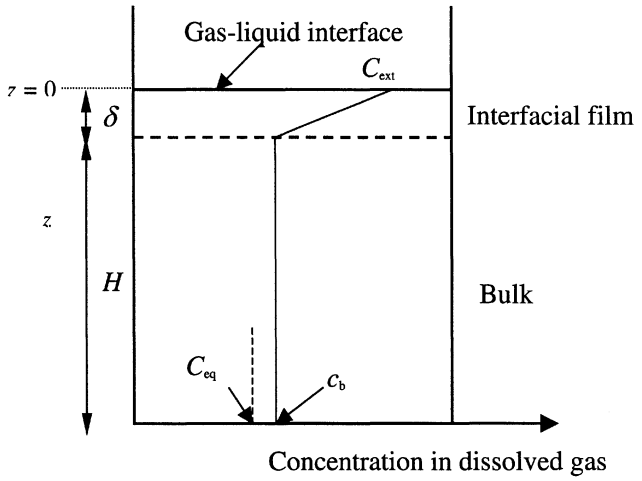

Figure 1. Crystallization reactor.

Processes

Gas Absorption. The gas absorption rate per unit volume $r(t)$ is expressed by the well-known relation (Mehta and Sharma, 1971; Sridharan and Sharma, 1976)

$$r(t) = k_L a\left(C_{\text{ext}} - c_b(t)\right) \tag{1}$$

where a is the mass transfer surface area per volume of liquid, and k_L the mass-transfer coefficient. In the experiments reported here, $k_L a$ ranges between 0.0001 and 0.005 s^{-1}.

Mass Transport in the Interfacial Layer. In the two-film theory, the interfacial layer thickness is obtained from the relation

$$\delta = \frac{D_G a}{k_L a} \tag{2}$$

in which D_G is the dissolved gas diffusivity. For instance, δ ranges between 44 and 126 μm in Wachi and Jones (1991b) and between 10 and 50 μm in Herri et al. (1999). Thus, the interfacial layer is very thin compared to the usual height of the liquid in the reactor (0.2 m).

Concentration is maintained at value C_{ext} by the gas–liquid equilibrium at the external interface. Crystallization occurs because C_{ext} is greater than C_{eq}, the equilibrium concentration in the presence of crystals. Concentration in the bulk, c_b, is proved to be close to C_{eq}, at least at late stages of the crystallization process. This is proved by simulations in Skovborg and Rasmussen (1994) and Herri et al. (1999), and will be discussed later in this text. This means that supersaturation sharply decreases throughout the film layer. In gas–liquid precipitation experiments, visual observations clearly show that nucleation mainly takes place in the interfacial film from which the nucleated crystals are then transferred to the bulk, where they go on growing. According to the authors, this transfer process is differently described. Wachi and Jones (1991a) attribute it to Stokes-Einstein diffusion, whereas Englezos et al. (1987a,b) consider that nuclei appear in the film and are instantaneously transferred to the bulk as soon as supersaturation conditions are created. We propose here a discussion on the interlayer transfer process by taking Stokes diffusion, settling (or floating), and crystal growth into account.

The Stokes-Einstein diffusion coefficient D_P of a spherical particle of diameter D' is given by the relation

$$D_P = \frac{kT}{3\pi\eta_L D'} \tag{3}$$

in which T is the temperature, η_L is the dynamic viscosity of the liquid medium, and k is the Boltzmann constant.

Particles immersed in a fluid move downwards (settling) or upwards (floating), so they are, respectively, denser (case of calcium carbonate in water) or lighter (case of methane hydrate) than the fluid medium. In both cases, their limit velocity w is given by the expression

$$w = \frac{D'^2 g|\Delta\rho|}{18\eta_L} \tag{4}$$

in which g denotes the gravity and $|\Delta\rho|$ the absolute value of the density difference between the solid and liquid phase.

The relative importance of Stokes-Einstein diffusion and settling (or floating) can be judged from the corresponding particle fluxes, that is, respectively

$$J_P = -D_P \frac{\partial n'}{\partial z} \tag{5}$$

and

$$J_{S/F} = n' \cdot w \tag{6}$$

From dimensional analysis it follows that

$$\frac{J_P}{J_{S/F}} \cong \frac{6kT}{\pi g} \frac{1}{D'^3 |\Delta\rho|} \frac{1}{\delta} \tag{7}$$

For the experimental systems under consideration (Herri et al., 1999; Wachi and Jones, 1991a,b), the typical parameter values $\{T,\ \delta,\ |\Delta\rho|\}$ are, respectively, {275 K, 30 μm, 88 kg$\cdot$m^{-3}} for methane hydrate in water and {293 K, 80 μm, 1,700 kg$\cdot$m^{-3}} for calcium carbonate in water. Stokes-Einstein diffusion is preponderant for $D' < 0.65$ μm in the first case, and $D' < 0.18$ μm in the second case. These grain sizes are reached in about 19 s (growth rate $G \approx 2$ μm$\cdot$min^{-1}) and 36 s (growth rate $G \approx 0.3$ μm$\cdot$min^{-1}), respectively. The sedimentation (or floating) times: $t_{S/F}$ ($t_{S/F} = \delta \cdot w^{-1}$) are equal to 1,400 s and 2,600 s, respectively.

From the order of magnitude of these values, it appears that, once a crystal is nucleated in the interfacial film, it rapidly reaches a size for which diffusion is negligible; this means that its motion is essentially ruled by sedimentation or flotation. In both cases, most crystals are nucleated at the gas–solid boundary, where supersaturation is maximum. However, their further behavior is different according to their density:

(1) Crystals denser than water fall downwards and leave the interfacial layer to enter the bulk; their size at this moment and their residence time in the film can be obtained from the equality between *sedimentation time*: t_S ($t_S = \delta \cdot w^{-1}$) and *growth time* t_G ($t_G = G^{-1} \cdot D'$). In the case of calcium carbonate in water, this calculation gives a residence time of 152 s and a size of 0.72 μm.

(2) Crystals lighter than water tend to float and move upwards to the gas–liquid interface, where they go on growing. Their transfer to the bulk zone is probably due to entrainment by the bulk flow; however, their transfer should occur only beyond a minimum size (Taniguchi et al., 1996)

Crystallization Steps. The crystallization steps are presented independently of the reactor zone in which they occur. Classic assumptions are taken for the kinetic laws of the different crystallization steps

Linear Growth Rate G:

$$G = k_g \sigma^p \tag{8}$$

in which σ ($\sigma = (c/C_{\text{eq}}) - 1$) is the relative supersaturation level in the considered medium; C_{eq} is the equilibrium concentration in the presence of the solid phase; constant k_g is assumed to be independent of the crystal diameter D (MacCabe simplification), although possibly dependent on the stirring rate, p is a constant of typical values 1 or 2 (Garside, 1985; Dirksen and Ring, 1991).

Primary Nucleation Rate B_1. The production rate of primary nuclei per unit volume is expressed according to the classic expression (Nielsen, 1964)

$$B_1 \propto e^{-(\beta_n / \ln(1+\sigma)^2)} \tag{9}$$

or more simply by

$$B_1 = k_1 \sigma^{n_1} \tag{10}$$

in which k_1 and β_n are positive constants and n_1, a positive exponent, can commonly take relatively high values (5 to 10). Nuclei are supposed to be created at a zero initial size.

Secondary Nucleation Rate B_2. The production rate of secondary nuclei per unit volume is expressed by (Garside, 1985)

$$B_2 = k_2 \sigma^m m_2 \tag{11}$$

in which k_2 is a constant, generally dependent on agitation, m is a positive exponent ranging from zero (purely mechanical origin of the nuclei) to relatively low values (typically 2 to 3; case of "true" secondary nucleation) (Garside, 1985); m_2 denotes the second-order moment of the diameter distribution (proportional to the crystal surface area per unit volume of the medium). Proportionality between B_2 and m_2 corresponds to a situation of relatively low concentrations in the solid, as observed in the reported experiments. As before, for primary nucleation, the initial size of the secondary nuclei is assumed to be zero.

Agglomeration. The agglomeration kernels depend both on agitation and supersaturation (Hounslow et al., 1998). In this article, agglomeration will not be considered in a very rigorous and precise way, but only the trends it induces will be investigated. The role of agglomeration in the different crystal population balances will be represented by an additive term A_{agg}, which will be expressed later on.

Model dynamic equations

In this section we present the general dynamic equations that describe the time evolution of the system, particularly of the concentration in dissolved gas and of the crystal density function and the simplification that can be assumed in each zone.

Mass Balance. In any point of the two zones, the mass balance in dissolved gas is expressed by the general partial derivative equation

$$\frac{\partial c}{\partial t} = -\frac{k_\upsilon m_2}{\upsilon_{\text{mol}}} G - \frac{\partial J_D}{\partial z} \tag{12}$$

where J_D is the molar flux of the dissolved gas, m_2 the second-order moment of the crystal distribution, υ_{mol} the solid molar volume, and k_υ a crystal shape constant ($k_\upsilon = \pi/2$ for spherical particles).

i. Bulk Zone. As it is supposed that the bulk zone is perfectly mixed, Eq. 12 is not relevant, at least in the present form, and it should be replaced for the following global balance using Eq. 1

$$\frac{dc_b}{dt} = k_L a(C_{\text{ext}} - c_b) - \frac{k_v m_{2b}}{v_{\text{mol}}} G_b \tag{13}$$

ii. Interfacial Layer. As is common in the framework of the film model (Welty et al., 1969; Beek et al., 1975), comparison between the gas absorption flow rate and the amount of gas actually consumed in the interfacial layer can suggest simplifications.

Ratio γ between the two flow rates is given by

$$\gamma = \frac{k_L a(C_{\text{ext}} - c_b)H}{\frac{k_v m'_2}{v_{\text{mol}}} G'\delta} \tag{14}$$

Denoting ϕ' the volume fraction of the solid and $\overline{D}'$ the crystal mean diameter in the film, assuming $C_{\text{ext}} \gg c_b$, and $a \approx 1/H$, and using Eq. 2, we obtain an approximate expression of γ

$$\gamma = \frac{D_G}{3\phi' G'} \overline{D}' \frac{1}{\delta^2} C_{\text{ext}} v_{\text{mol}} \tag{15}$$

The parameter typical values $\{\overline{D}', \delta, G', C_{\text{ext}} v_{\text{mol}}\}$ are, respectively:

$\{5\ \mu\text{m}, 30\ \mu\text{m}, 2\ \mu\text{m}\cdot\text{min}^{-1}, 7.2\times10^{-3}\}$ for methane hydrate in water

$\{1\ \mu\text{m}, 80\ \mu\text{m}, 0.3\ \mu\text{m}\cdot\text{min}^{-1}, 1.8\times10^{-4}\}$ *for calcium* carbonate in water.

In both systems, common values are taken for D_G (5×10^{-9} $\text{m}^2\cdot\text{s}^{-1}$) and ϕ' (0.01).

The corresponding calculated values of γ are 200 for methane hydrate in water and 11 for calcium carbonate in water. Due to the uncertainty of the different parameters, these values are not accurate. They give a realistic estimation of γ, however, and prove that crystallization weakly affects mass transfer in the interfacial layer; consequently, from Eq. 12, it follows that a linear profile of concentration ranging between C_{ext} and C_b can be assumed in the interfacial layer at the steady state.

Remark. For the sake of simplicity, the role of possible chemical steps in the interfacial layer mass balance has been overlooked; this is a common assumption in the case of the gas hydrate crystallization; for other systems, it can be considered as the borderline, but plausible, case of rapid reversible reactions. It would be quite possible to take the kinetics of the chemical steps into account when they exist; however, each case would be a particular one, for which the present approach can give hints.

Crystal Population Balances. The crystal population balance is expressed by the general partial derivative equation

$$\frac{\partial n}{\partial t} + G\frac{\partial n}{\partial D} - B_1 - B_2 + \frac{\partial J}{\partial z} - A_{ag} = 0 \tag{16}$$

where the population density function n depends on diameter D, time t, and height z. Flux J refers to the circulation of the particles in the system ($J_{S/F}$, J_P, as mentioned before, or convection flux).

i. Interfacial Layer. We propose two simplifying assumptions for the interfacial layer.

- Steady state: this is justified by the small extension of this layer and its incessant exchange with the gaseous atmosphere and the liquid bulk.
- Linear profile of concentration in dissolved gas and negligible crystallization processes (that is, growth, agglomeration, and secondary nucleation) except, of course, primary nucleation: this is justified by the calculated γ values and the possibilities of permanent exchange with the bulk.

Taking into account too that particles nucleated in the film are rapidly transferred to the bulk (either by sedimentation or by flow entrainment), their starting size in the bulk is probably a bit dispersed and small. This is the reason why we gave up calculating it accurately, and we restrict the role of the interfacial film to an external source of nuclei that feeds the bulk of the reactor.

Averaged nucleation rate $\overline{B'_1}$ can be calculated from integration of Eq. 10 over the film to give

$$\overline{B'_1} = \frac{k_1}{n_1+1} \frac{\sigma_{\text{ext}}^{n_1+1} - \sigma_b^{n_1+1}}{\sigma_{\text{ext}} - \sigma_b} \tag{17}$$

where σ_{ext} and σ_b are the supersaturation level at the gas–liquid and at the two-layer interface, respectively.

ii. Bulk Zone. Population balance is deduced from the general equation (Eq. 16); however, taking into account the bulk homogeneity and the feed in nuclei from the interfacial film, it follows

$$\frac{\partial n_b(D,t)}{\partial t} + G_b\frac{\partial n_b(D,t)}{\partial D} - \frac{\delta}{H}\overline{B'_1} - B_{1b} - B_{2b} - A_{\text{agg}_b}(D) = 0 \tag{18}$$

In the classic crystal population balance equations (Randolph and Larson, 1988), particularly in the framework of the MSMPR model, nuclei are generally assumed to be generated at initial zero size. This simplification is certainly valid for nuclei created by primary nucleation (B_{1b}) or "true" secondary nucleation (B_{2b}; Eq. 11, with m different from 0). According to previous discussions in this text, however, it is certainly questionable when the nuclei are produced in the interfacial film and then transferred to the bulk (term $\overline{B'_1}$). We propose to consider a nonnecessarily zero initial size (D'_{0b}) for these nuclei.

Moment Equations. The first three moments of the crystal size distribution by number in the bulk are

$$m_{0b} = \int n_b(D)\cdot dD \tag{19}$$

$$m_{1b} = \int n_b(D)\cdot D\cdot dD \tag{20}$$

$$m_{2b} = \int n_b(D) D^2\cdot dD \tag{21}$$

The partial derivative equation (Eq. 18) results in the following moment equations

$$\frac{dm_{0b}}{dt} = \frac{\delta}{H}\overline{B'_1} + B_{1b} + B_{2b} - \frac{K_{agg}}{2}m_{0b}^2 \quad (22)$$

$$\frac{dm_{1b}}{dt} = G_b m_{0b} + \frac{\delta}{H}\overline{B'_1}D'_{0b} - \beta_1 K_{agg} m_{0b} m_{1b} \quad (23)$$

$$\frac{dm_{2b}}{dt} = 2G_b m_{1b} + \frac{\delta}{H}\overline{B'_1}D'^2_{0b} - \beta_2 K_{agg} m_{0b} m_{2b} \quad (24)$$

The presence of $\overline{B'_1}$ terms in Eqs. 23 and 24 derives from the possibility of nuclei of nonzero size as said earlier. The last terms of the lefthand side of these equations are due to the contribution of agglomeration (K_{agg}, β_1, β_2 are positive constants). These are approximate expressions that assume constant agglomeration kernel and take into account the experimental shape of the crystal-size distribution. This simplification has been already introduced and validated by Herri et al. (1999) in the case of crystallization of methane hydrate.

Asymptotic solution to the problem

Solving Eqs. 13, 22–24 requires numerical integration, which presents no particular difficulty; however, it is not straightforward (Englezos et al., 1987; Wachi and Jones, 1991a,b; Herri et al., 1999). Sensitivity to the system parameters clearly appears from these results, but they cannot be described in simple words. We will prove here that the asymptotic solution of the problem can be found in an analytical form, the parameters of which are the characteristics of the system and the processes.

Mathematical Procedure. The calculation procedure begins with the mass-balance equation

$$\frac{dc_b}{dt} = k_L a(C_{ext} - c_b) - \frac{k_v m_{2b}}{v_{mol}} G_b \quad (13)$$

In the presence of crystals, the thermodynamic variance of the present solid–liquid–gas system is equal to 1. This means that, at the given temperature, equilibrium conditions are determined, particularly pressure and temperature. If, like here, external pressure is fixed at a value P_{ext} higher than the equilibrium value P_{eq} (or equivalently, $C_{ext} > C_{eq}$), the system continuously adsorbs gas to create new crystals. Thus, m_{2b} continuously increases and is assumed to be asymptotically proportional to t^{α}, where α is a positive exponent.

Remark. In the presence of agglomeration, the situation is more complex and will be examined later on. For the moment, we assume that K_{agg} is zero.

As in Eq. 13, product $G_b m_{2b}$ should keep finite values, where G_b necessarily tends to zero, and, thus, is of the form

$$G_b = Kt^{-\alpha} \quad (25)$$

Thus, from Eq. 8, c_b tends asymptotically to C_{eq}.

Putting these asymptotic values into Eq. 13 gives

$$m_{2b} = \frac{A}{K}t^{\alpha} \quad (26)$$

with

$$A = \frac{k_L a C_{eq} \sigma_{ext} v_{mol}}{k_v} \quad (27)$$

The asymptotic value of the nucleation rate in the film is

$$\overline{B'_1} = \frac{k_1}{n_1 + 1}\sigma_{ext}^{n_1} \quad (28)$$

The next steps of the procedure consist of:

(1) Putting m_{2b} and G_b into Eq. 24 and deriving m_{1b};

(2) Putting m_{1b} and G_b into Eq. 23 and deriving m_{0b};

(3) Putting m_{0b} into Eq. 22 and identifying α and K;

(4) Expressing the different moments and characteristics of the crystal population (particle number and mean diameter).

Typical Cases. The previous procedure can be applied to different situations of rate-determining crystallization steps.

• *Film Nucleation and Bulk Growth*. In this case, the basic assumption is that nucleation only occurs in the film and is negligible in the bulk (due to too low supersaturation in the bulk).

Equations 24, 23, 22 can be, respectively, simplified in

$$\frac{dm_{2b}}{dt} = 2G_b m_{1b} + \frac{\delta}{H}\overline{B'_1}D'^2_{0b} \qquad \frac{dm_{1b}}{dt} = G_b m_{0b} + \frac{\delta}{H}\overline{B'_1}D'_{0b}$$

$$\frac{dm_{0b}}{dt} = \frac{\delta}{H}\overline{B'_1}$$

Applying the previous procedure successively gives

$$m_{1b} = \frac{A}{2K^2}\alpha t^{2\alpha-1} - \frac{\delta}{HK}\overline{B'_1}D'^2_{0b}t^{\alpha} \quad (29)$$

$$m_{0b} = \frac{A}{2K^3}\alpha(2\alpha-1)t^{3\alpha-2} - \frac{\delta}{HK^2}\overline{B'_1}D'^2_{0b}t^{2\alpha-1} - \frac{\delta}{H}\overline{B'_1}D'_{0b}t^{\alpha} \quad (30)$$

$$1 = \frac{AH}{2\delta K^3}\frac{n_1+1}{k_1\sigma_{ext}^{n_1}}\alpha(2\alpha-1)(3\alpha-2)t^{3\alpha-3} - \frac{1}{K^2}(2\alpha-1)D'^2_{0b}t^{2\alpha-2} - \frac{1}{K}D'_{0b}\alpha t^{\alpha-1} \quad (31)$$

The values of α and K are obtained from identification according to the powers of t in Eq. 31: $\alpha = 1$ and K is a root of the equation

$$1 = \frac{AH}{2\delta K^3}\frac{n_1+1}{k_1\sigma_{ext}^{n_1}} - \frac{1}{K^2}D'^2_{0b} - \frac{1}{K}D'_{0b}$$

If the initial size of the nuclei transferred to the bulk can be neglected, then also using Eqs. 2 and 27, we can express, respectively, K, N_b, the asymptotic number of crystals in the

bulk and $\overline{D}_b$ their mean size

$$K = \left(\frac{(k_L a)^2 C_{eq} \upsilon_{mol} H}{2 D_G a k_\upsilon} \frac{n_1 + 1}{k_1 \sigma_{ext}^{n_1 - 1}} \right)^{1/3} \tag{32}$$

$$N_b = \frac{D_G a k_1 \sigma_{ext}^{n_1}}{(k_L a) H (n_1 + 1)} t \tag{33}$$

$$\overline{D}_b = \left(\frac{(k_L a)^2 C_{eq} \upsilon_{mol} H}{2 D_G a k_\upsilon} \frac{n_1 + 1}{k_1 \sigma_{ext}^{n_1 - 1}} \right)^{1/3} \tag{34}$$

Consequently, in this case, the number of crystals increases linearly and their mean size keeps constant.

Remark. The asymptotic steadiness of $\overline{D}_b$ was also observed in the simulation results of Herri et al. (1999) within similar model assumptions.

• *Film Nucleation, Bulk Growth, and Bulk Secondary Nucleation*. In this case, we still consider film nucleation and bulk growth as rate-determining; however, we also take into account secondary nucleation, which could play a part because of the continuously increasing surface area of the crystals. As previously we consider that $D'_{b0} = 0$.

Equations 24, 23, 22, respectively, can be simplified in

$$m_{1b} = \frac{A}{2K^2} \alpha t^{2\alpha - 1} \tag{35}$$

$$m_{0b} = \frac{A}{2K^3} \alpha (2\alpha - 1)^{3\alpha - 2} \tag{36}$$

$$\frac{k_1 \sigma_{ext}^n}{n_1 + 1} \frac{\delta}{H} + B_{2b} = \frac{A}{2K^3} \alpha (2\alpha - 1)(3\alpha - 2) t^{3\alpha - 3} \tag{37}$$

From Eqs. 8 and 11, it follows that

$$B_{2b} = k_2 \left(\frac{G_b}{k_G} \right)^{m/p} m_{2b} \tag{38}$$

Using Eq. 8 and the expressions of the asymptotic variation of G and m_{2b} with time (Eqs. 25 and 26), we transform Eq. 37 in

$$\frac{k_1 \sigma_{ext}^n}{n_1 + 1} \frac{\delta}{H} + A \frac{k_2}{k_G^{m/p}} K^{(m/p) - 1} t^{(1 - (m/p))\alpha} = \frac{A}{2K^3} \alpha (2\alpha - 1)(3\alpha - 2) t^{3\alpha - 3} \tag{39}$$

Identification according to the powers of t is a little more complicated than previously and boils down to the following two cases:

(1) $3\alpha - 3 = 0$, that is, $\alpha = 1$; however, with $m > p$, this latter condition shows that the secondary nucleation rate should depend more on supersaturation than growth rate. This behavior is rather common for "true" secondary nucleation. If these conditions are fulfilled, case 1 is asymptotically similar to the situation of film nucleation-growth bulk, which was discussed before (Eqs. 32–34). This means that asymptotically bulk "true" secondary nucleation is less active than film primary nucleation.

(2) $(1 - (m/p))\alpha = 3\alpha - 3$, that is, $\alpha = 3/(2 + m/p)$; however, with $m < p$, as explained in the previous section, this latter condition is not frequently met for "true" secondary nucleation. However, it is, of course, observed in the case of purely mechanical nuclei generation ($m = 0$).

The respective expressions of K, and asymptotic N_b and $\overline{D}_b$, are

$$K = \left[\frac{k_G^{m/p}}{2k_2} \alpha (2\alpha - 1)(3\alpha - 2) \right]^{\alpha/3}$$

$$N_b = \frac{k_L a C_{eq} \sigma_{ext} \upsilon_{mol}}{2k_\upsilon [\alpha (2\alpha - 1)]^{\alpha - 1} \left[\frac{k_G^{m/p}}{2k_2} (3\alpha - 2) \right]^{\alpha}} t^{3\alpha - 2}$$

$$\overline{D}_b = \frac{\left[\frac{k_G^{m/p}}{2k_2} \alpha (3\alpha - 2) \right]^{\alpha/3}}{(2\alpha - 1)^{1 - (\alpha/3)}} t^{1 - \alpha}$$

In the case of the secondary nucleation of purely mechanical origin ($m = 0$; $\alpha = 3/2$), these expressions become

$$K = \left(\frac{15}{4k_2} \right)^{1/2} \tag{40}$$

$$N_b = \frac{3 k_L a C_{eq} \sigma_{ext} \upsilon_{mol}}{2 k_\upsilon^{1/2} \left[\frac{15}{4k_2} \right]^{3/2}} t^{5/2} \tag{41}$$

$$\overline{D}_b = \frac{\left[\frac{15}{16 k_2} \right]^{1/2}}{t^{1/2}} \tag{42}$$

Thus, in this case, the mean diameter asymptotically decreases with time.

• *Role of Bulk Agglomeration.* We will envisage only the cases of simultaneous film primary nucleation, bulk crystal growth, and bulk agglomeration. The relevant equations are

$$\frac{dc_b}{dt} = k_L a (C_{ext} - c_b) - \frac{k_\upsilon m_{2b}}{\upsilon_{mol}} G_b \tag{13}$$

$$\frac{dm_{0b}}{dt} = \frac{\delta}{H} \overline{B}'_1 - \frac{K_{agg}}{2} m_{0b}^2 \tag{43}$$

$$\frac{dm_{1b}}{dt} = G_b m_{0b} - \beta_1 K_{agg} m_{0b} m_{1b} \tag{44}$$

$$\frac{dm_{2b}}{dt} = 2 G_b m_{1b} - \beta_2 K_{agg} m_{0b} m_{2b} \tag{45}$$

The case of zero K_{agg} has been studied earlier in this text (Eqs. 32–34) and is characterized by asymptotic linear variation of the crystal number and constant particle diameter.

If K_{agg} is different from zero, agglomeration takes place. From a mathematical point of view, the differential system (Eqs. 13, 43–45) admits an asymptotic steady state for which c_b is different from C_{eq} ($C_{ext} > c_b > C_{eq}$). Consequently, this is not an equilibrium state, although the first three moments become constant; however, gas absorption goes on. In this

text, we will not present further developments concerning this steady state, because, in the absence of experimental evidence, it would be essentially academic.

However, considering weak agglomeration—low value of K_{agg}, for instance—an approximate solution to Eqs. 43–45 can be found easily using a perturbation procedure. This solution is valid at intermediate stages of the process, and due to the approximation it involves, should be considered only as regards to the trend it is responsible for in the evolution of the system time. Approximate values of crystal number and mean diameter are

$$N_b^{agg}(t) = N_b^0(t)\left(1 - K_{agg}\frac{\delta\overline{B_1'}}{6H}t^2\right) \tag{46}$$

$$\overline{D}_b^{agg}(t) = \overline{D}_b^0\left[1 + K_{agg}\frac{\delta\overline{B_1'}}{H}\left(1 - \frac{2}{3}\beta_1\right)t^2\right] \tag{47}$$

where the supercript *agg* refers to the introduction of agglomeration; the superscript 0 refers to the absence of agglomeration (Eqs. 33 and 34).

It clearly appears that, as expected, agglomeration reduces the crystal number, but increases their mean diameter, provided $\beta_1 < 1.5$ [$\beta_1 = 0.262$ in Herri et al. (1999)].

Comparison with Experimental Data

Previous theoretical results are now examined in the framework of the already mentioned experimental studies: calcium carbonate precipitation (Wachi and Jones, 1991a,b) and methane hydrate crystallization (Herri et al., 1999; Pic et al., 2001).

The former case will be less commented on than the latter for different reasons:

(1) The existence of a chemical reaction in the film, which is not considered extensively in the present model (see previous Remark); however, the procedure should not be questioned.

(2) Nonconstant parameters (pH, in particular) throughout the experimental process, which could induce time-evolution of some parameters (not considered within the model).

(3) Lack of experimental results; in this respect, the methane hydrate system, which was studied by the authors of the present article, is very rich in data because of the instrumentation of the reactor with an optical sensor for *in situ* particle-size determinations (Herri et al., 1999; Pic et al., 2001).

Agreement between theory and experiment will be discussed in several aspects.

• *Time Evolution of Crystal Number and Mean Diameter at Different Stirring Rates*. In Figure 2, we recall experimental results obtained by us (Herri et al., 1999) on methane hydrate crystallization. According to the stirring rate, the time evolution of the crystal density and the mean diameter are quite different.

Concerning the asymptotic law of variation with the time of the crystal mean diameter and crystal number, if we represent them using, respectively, a law in t^{β} and a law in t^{ϵ}, we obtain the following results:

(1) $\beta < 0$ and $\epsilon > 1$ at high stirring-rate values (500 rpm).

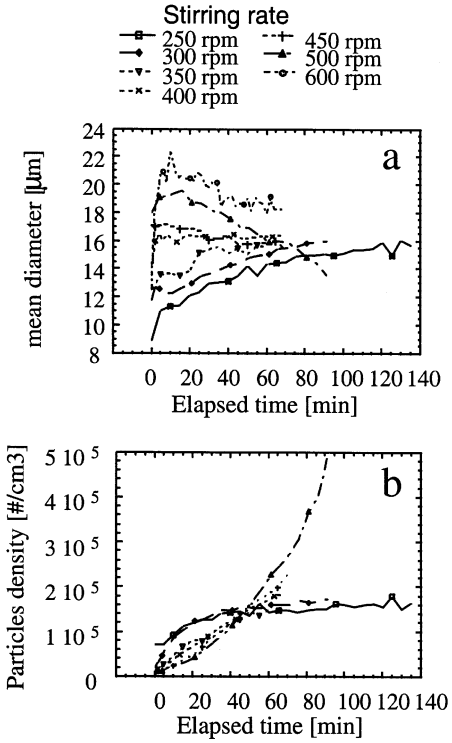

Figure 2. (a) Time evolution of crystal mean diameter and (b) number per unit volume at different stirring rates during methane hydrate crystallization at 30 bars and 1°C (experimental results from Herri et al., 1999).

(2) $\beta = 0$ and $\epsilon = 1$ at intermediate stirring-rate values (400 rpm).

(3) $\beta > 0$ and $\epsilon < 1$ at low stirring-rate values (250 rpm).

These results are quite consistent with the different theoretical possibilities we considered before.

(1) The case of film nucleation, bulk crystal growth, and secondary nucleation (with $m/p \approx 1/2$ at 500 rpm); this latter assumption is particularly plausible, because a high stirring rate can result in crystal erosion or attrition.

(2) The case of film nucleation and bulk crystal growth (at these moderate stirring rate values, agglomeration and attrition have opposite, somewhat balanced effects).

(3) The case of film nucleation, bulk crystal growth, and agglomeration (at the lowest stirring rate, agglomeration overcomes fragmentation).

The transition between case 1 and case 2 when the stirring rate is decreasing can be considered from a theoretical point of view by comparing the N_b values in the two cases (Eqs. 33 and 41). It appears that crystal production by attrition should outweigh primary nucleation beyond a certain time, t_l, which is obtained from the ratio of the respective N_b expressions

$$t_l \approx \left(\frac{k_1 D_G}{(4k_2)^{3/2} k_L^2 a}\sigma_{ext}^{n_1 - 1}\right)^{2/3} \tag{48}$$

In this expression, k_L, a, and probably k_2 are the most dependent on the stirring rate and increasing functions. This means that the predominance of attrition should be observed

earlier at a higher stirring rate. This is precisely what is observed.

The results from Wachi and Jones (1991b) also clearly show a slight increase in the mean crystal diameter to a possible maximum. No data on particle number are available. This behavior is quite consistent with the mechanism of film nucleation and bulk crystal growth perturbed by agglomeration (which is actually mentioned by the authors).

• *Influence of Stirring Rate on the Mean Crystal Diameter.* We consider only experiments in which primary nucleation

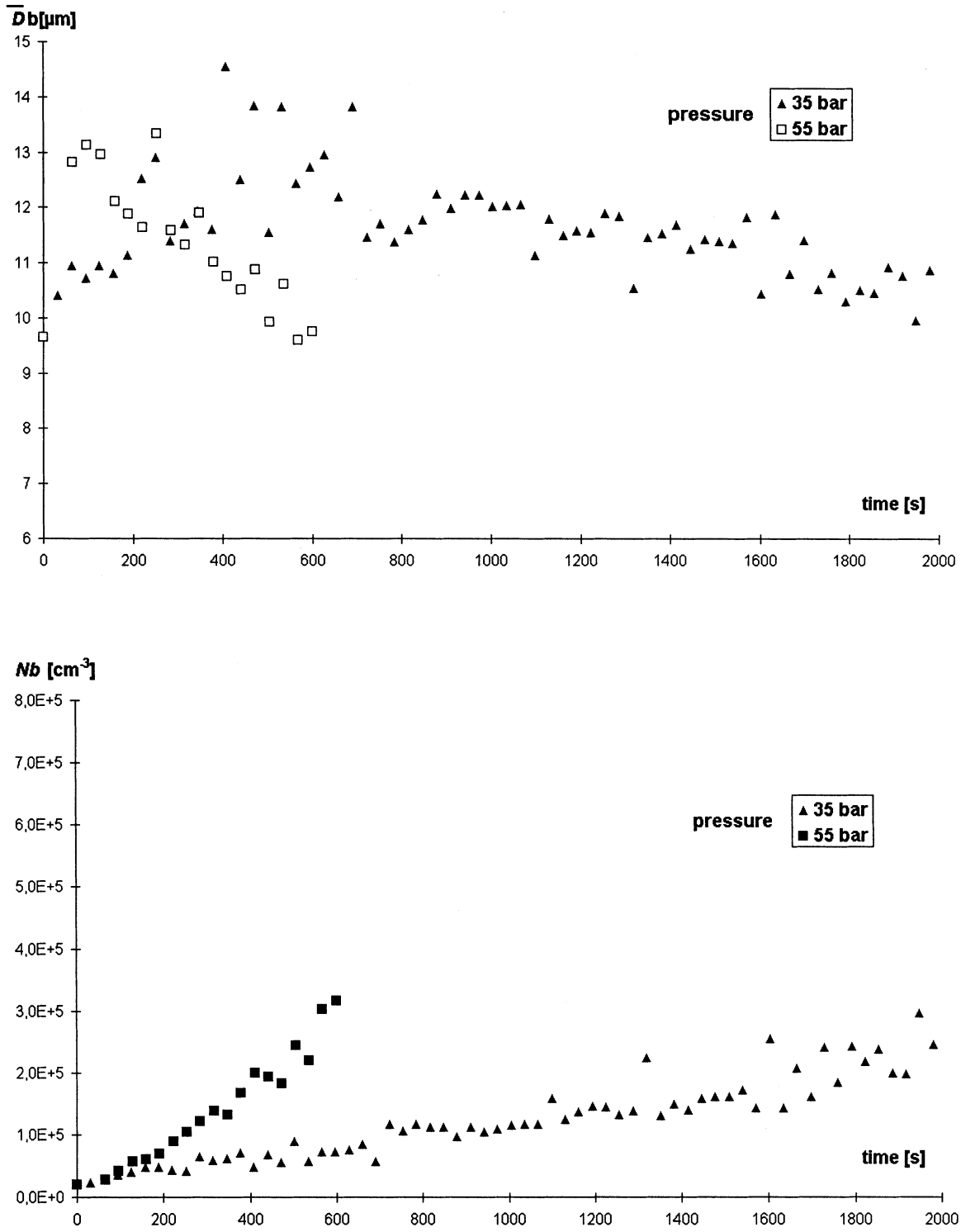

Figure 3. Effect of supersaturation (via methane hydrate pressure) on crystal mean diameter and total number (stirring rate: 300 rpm) (experimental results from Pic et al., 2001).

and crystal growth are preponderant, that is to say, with constant asymptotic mean diameter $\overline{D}_b$.

From Figure 2, it appears that $\overline{D}_b$ increases with the stirring rate in the range (350–450 rpm), for which $\overline{D}_b$ is nearly independent of time. The same conclusions can be derived from the results of Jones et al. (1992) on asymptotic mean diameter of calcium carbonate.

The previous model predicts the following asymptotic value for this diameter

$$\overline{D}_b = \left(\frac{(k_L a)^2 C_{\text{eq}} v_{\text{mol}} H}{2 D_G a k_v} \frac{n_1 + 1}{k_1 \sigma_{\text{ext}}^{n_1 - 1}} \right)^{1/3} \tag{34}$$

In this expression, the most dependent factor on the stirring rate is k_L, which is known to be an increasing function (Wachi and Jones, 1991b; Herri et al., 1999). This is quite consistent with the experimental results and with the simulation results of Herri et al. (1999).

• *Influence of Supersaturation on the Mean Crystal Diameter and Number Variation with Time*. We comment now on results obtained by us and extensively presented in Pic et al. (2001). They also concern methane hydrate crystallization in batch conditions, but in noticeably different hydrodynamic conditions. Figure 3 clearly shows that at a pressure of 3.5 MPa, $\overline{D}_b$ is practically constant and N_b is slowly and linearly increasing with time, whereas at 5.5 MPa, N_b increases as t^{ϵ}, with $\epsilon > 1$, and $\overline{D}_b$ decreases. In agreement with the N_b time variation (as predicted by the models), we consider that $\overline{D}_b$ varies as t^{β} with $\beta < 0$. The stirring rate is the same in both cases (300 rpm). This type of transition was observed earlier, but at an increasing stirring rate and constant supersaturation. Equation 48 can be examined again to determine the respective weights of attrition and primary nucleation at different supersaturation levels; this gives

$$t_l \approx \sigma_{\text{ext}}^{2(n_1 - 1)/3} \tag{49}$$

Assuming that only σ_{ext} depends on the supersaturation, and as n_1 is expected to be higher than 1, this means that attrition should be preponderant at a lower supersaturation level; in fact, the opposite behavior is observed. At the moment, we do not have a definitive explanation for this discrepancy.

Conclusion

In this article, we proposed a new discussion on gas–liquid crystallization in the framework of two-film models. Assumptions and interpretations were systematically placed in the context of two experimental systems of reference. This led us to propose a simplified, but realistic, expression of the process dynamics in the form of a system of differential equation in dissolved gas concentration and crystal distribution moments. Instead of solving this system numerically, as several authors did, we proposed a general and easy procedure to obtain an asymptotic solution. According to the relevant crystallization processes (primary nucleation, secondary nucleation, crystal growth, agglomeration), the different asymptotic laws of crystal number and mean diameter vs. time are calculated and found in an analytical form in which the influence of different parameters (stirring rate, supersaturation) are quantitatively expressed. Using these predictions, we could interpret most of the data coming from calcium carbonate precipitation and methane hydrate crystallization. In this latter case, in particular, we confirmed the strong influence of the stirring rate, which is shown by the experiments, and we explained it through its action on agglomeration and fragmentation.

Literature Cited

Beek, W. J., K. M. Muttzall, and J. W. van Heuven, *Transport Phenomena*, Wiley, New York (1975).

Dirksen, J., and T. Ring, "Fundamentals of Crystallization: Kinetic Effects on Particle Size Distributions and Morphology," *Chem. Eng. Sci.*, **46**, 2389 (1991).

Englezos, P., N. Kalogerakis, P. D. Dholabai, and P. R. Bishnoi, "Kinetics of Formation of Methane and Ethane Gas Hydrates," *Chem. Eng. Sci.*, **42**, 2647 (1987a).

Englezos, P., N. Kalogerakis, P. D. Dholabai, and P. R. Bishnoi, "Kinetics of Gas Hydrate Formation from Mixtures of Methane and Ethane," *Chem. Eng. Sci.*, **42**, 2659 (1987b).

Garside, J., "Industrial Crystallization from Solution," *Chem. Eng. Sci.*, **40**, 3 (1985).

Herri, J. M., J. S. Pic, F. Gruy, and M. Cournil, "Methane Hydrate Crystallization Mechanism from In-Situ Particle Sizing," *AIChE J.*, **45**, 590 (1999).

Hounslow, M. J., A. S. Bramley, and W. R. Paterson, "Aggregation During Precipitation from Solution. A Pore Diffusion-Reaction Model for Calcium Oxalate Monohydrate," *J. Colloid Interface Sci.*, **203**, 383 (1998).

Jones, A. G., J. Hodtomsky, and Z. Li, "On the Effect of Liquid Mixing Rate on Primary Crystal Size During the Gas-Liquid Precipitation of Calcium Carbonate," *Chem. Eng. Sci.*, **47**, 3817 (1992).

Mehta, V. D., and M. M. Sharma, "Mass Transfer in Mechanically Agitated Gas-Liquid Contactors," *Chem. Eng. Sci.*, **26**, 461 (1971).

Nielsen, A. E., *Kinetics of Precipitation*, Pergamon Press, Oxford (1964).

Pic, J. S., J. M. Herri, and M. Cournil, "Experimental Influence of Kinetic Inhibitors on Methane Hydrate Particle Size Distribution During Batch Crystallization in Water," *Can. J. Chem. Eng.*, **79**, 374 (2001).

Randolph, A. D., and M. A. Larson, *Theory of Particulate Processes*, 2nd ed., Academic Press, New York (1988).

Sada, E., H. Kumazawa, and M. A. Butt, "Single Gas Absorption with Reaction in a Slurry Containing Fine Particles," *Chem. Eng. Sci.*, **32**, 1165 (1977).

Skovborg, P., and P. Rasmussen, "A Mass Transport Limited Model for the Growth of Methane and Ethane Gas Hydrates," *Chem. Eng. Sci.*, **49**, 1131 (1994).

Sridharan, K., and M. M. Sharma, "New Systems and Methods for the Measurement of Effective Interfacial Area and Mass Transfer Coefficients in Gas-Liquid Contactors," *Chem. Eng. Sci.*, **31**, 767 (1976).

Taniguchi, S., S. Kawaguchi, and A. Kikuchi, "Dispersion Characteristics of Small Buoyant Particles in a Gas Agitated Vessel," *ISIJ Int.*, **36**(Suppl.), 46 (1996).

Wachi, S., and A. G. Jones, "Effect of Gas-Liquid Mass Transfer on Crystal Size Distribution During the Batch Precipitation of Calcium Carbonate," *Chem. Eng. Sci.*, **46**, 3289 (1991a).

Wachi, S., and A. G. Jones, "Mass Transfer with Chemical Reaction and Precipitation," *Chem. Eng. Sci.*, **46**, 1027 (1991b).

Welty, J. R., C. E. Wicks, and R. E. Wilson, *Fundamentals of Momentum, Heat and Mass Transfer*, Wiley, New York (1969).

Manuscript received July 12, 2002, revision received Dec. 12, 2002, and final revision received Mar. 17, 2003.